

# High-speed roller/rail dynamics and thermodynamics considering surface roughness and revolution

Jian Xu<sup>1</sup>, Zhen Yang<sup>2</sup>, Xuefang Chang<sup>3</sup>, Qiang Li<sup>4</sup>

School of Mechanical and Electrical Engineering, North University of China, Taiyuan, 030051, P. R. China

<sup>1</sup>Corresponding author

E-mail: <sup>1</sup>zdp12\_0@126.com, <sup>2</sup>15803431078@163.com, <sup>3</sup>20080005@nuc.edu.cn, <sup>4</sup>liqiang12@nuc.edu.cn

Received 3 October 2025; accepted 27 October 2025; published online 22 December 2025

DOI <https://doi.org/10.21595/vp.2025.25495>



74th International Conference on Vibroengineering in Tashkent, Uzbekistan, November 27-29, 2025

Copyright © 2025. This is an open access article distributed under the Creative Commons Attribution License, which permits unrestricted use, distribution, and reproduction in any medium, provided the original work is properly cited.

**Abstract.** Considering rotation and not considering rotation, a calculation was conducted on the friction and wear between the sliding pair in a high-speed rotating machine using a plane of Ra6.3 and Ra3.2, indicating that Ra3.2 has advantages. In higher firing rate Gatling guns, the guide rail should be processed more finely and have a smaller roughness. The results demonstrate that the stress increases a lot when the bolt is surface rough, which is 11.5 % higher than the flat condition. The temperature of Ra6.3 is about 100° higher than the flat condition. It plays an important role in improving the service life of friction surfaces.

**Keywords:** reverse engineering, thermodynamic, sliding pair, surface roughness, rotation, sliding wear, RPM (round per minute).

## 1. Introduction

For a long period, the high-speed and high-speed motion of contacting friction pairs [1], due to the heat generated by friction, the temperature rise in the contact area, will cause the adhesion and wear phenomenon, which seriously affects the normal work of the friction pair.

The real engineering surface [2] is composed of a series of uneven bumps. Contact occurs only on a very small number of bumps on the surface. Because the contact surface is very small, these bumps bear a great load and will produce elastoplastic deformation. When the micro-convex bodies in a contact state undergo relative movement, a large amount of heat is generated between the contact interfaces. The uneven distribution of heat will seriously affect the mechanical and physical properties of the material, making the forces between the micro-convex bodies more complicated and exacerbating.

Xuesong Jin [3] analyzed the classic wheel-rail rolling contact theory model, conducted numerical calculations on the modern wheel-rail rolling contact model, and analyzed its advantages, disadvantages, applications, and future development. Fujin Xia [4] believes that dynamic wheel loads are related to the dynamic system elements of freight cars, tracks, and wheel-rail interactions. Wu B. [5] believes that when the wheels enter the low adhesion zone, the wheel-rail creep force significantly decreases. When the adhesion is restored, the creep force will suddenly increase. In addition, when the traction coefficient is greater than 0.1 at high speeds. Wang W. J. [6] proposed that the adhesion coefficient of the wheel-rail slowly and slightly decreases under dry conditions, up to 5 %. If encountering a water medium, it will significantly affect the adhesion of the wheel-track. Lin Chang-gang [7] and Yin X. F. [8] discussed the performance of components under random vibration, such as bearings and bridge structures, but we are not discussing random vibration.

In some cases, check the contact between the bolt cam part and the guide rail. Predict that these friction pairs will repeatedly move on a fixed road for a certain period, without knowing their stress and displacement states, as well as temperature.

## 2. Physical model of main roller/guide rail

To a high Gatling gun, according to the cycle [9] in Fig. 1, the bolt group is constrained by the main roller, constrained by the curve groove in space, and rotates in space. The bolt cam part is shown as Fig. 2.

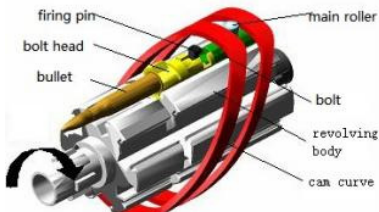


Fig. 1. Gatling mechanism

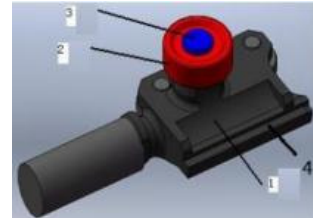


Fig. 2. Bolt cam part: 1 – main bolt, 2 – main roller, 3 – axis, 4 – sliding pair

## 3. Different firing rates for gatling gun

### 3.1. Regardless of rotational state

The bolt group is shown in Fig. 3, and the  $(x_0, y_0)$  is the central position of the bolt group and  $h = 30$  mm and  $b = 80$  mm,  $c = 60$  mm.

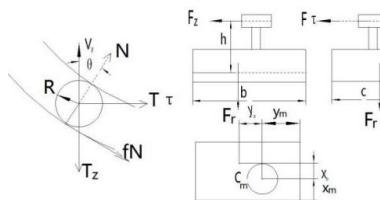


Fig. 3.  $x_0, y_0$  of the main roller to bolt cam part without rotational state

It is said that it is rotating, it can be seen that  $F_\tau$  acts laterally and reverses the movement set to the left:

$$F_z = N(\cos\theta - f\sin\theta), \quad (1)$$

$$F_\tau = N(\sin\theta + f\cos\theta). \quad (2)$$

Put the and project in the working part movement direction and form the active push force  $F_z$  of as Eq. (1) and the cross direction force  $F_\tau$  as Eq. (2) which is vertical to the movement direction [12-14].

### 3.2. Considering rotating state

If we consider the rotation of the main roller group, the bolt group is shown as Fig. 4.

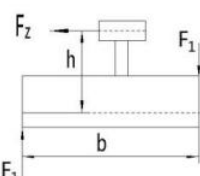


Fig. 4. F1's calculation

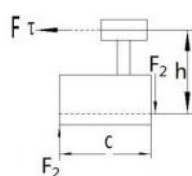


Fig. 5. F2's calculation

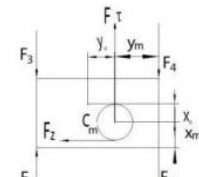


Fig. 6. F3 and F4's calculations

Except for friction force due to inertia force, other force, and their layout can be sketched in Figs. 4-6. And in these figures, the  $F_1$ ,  $F_2$ ,  $F_3$  and  $F_4$  are calculated as paper [9].

### 3.3. Dynamics equation of the main roller group

Considering rotation and non rotation, push all the force to its longitudinal direction and get the differential equation, and the symbols are as described in paper [9]:

$$ma = F_Z - 2fF_1 - 2fF_2 - 2fF_3 - 2fF_4 - K(fF_r + fF_g) - fF_\tau. \quad (3)$$

Suppose that  $x_0 \in (-21 21)$ ,  $y_0 \in (-31 31)$ . Set with the 10 Gatling guns and set with rotational variable, and get rpm  $\in (3300 10000)$ . Study on the layout of the main roller on the body, affects the relative position of the size  $(x_0, y_0)$  and the direction is to look at the main roller  $N$  and effects like in Table 1 and Fig. 7-9.

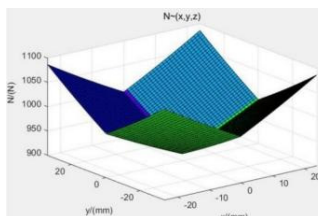


Fig. 7. Main force of 3300 rpm

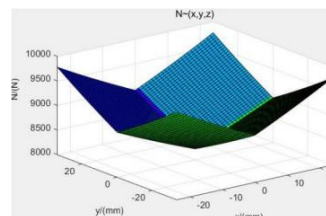


Fig. 8. Main force of 10000 rpm

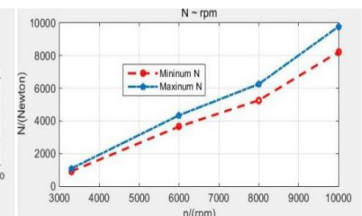


Fig. 9. The min and max  $N$  to rpm

### 4. Modeling rough surface

Reconstruct the surface roughness in UG [10] by reverse engineering technology. If Ra is 6.3 um, the surface is shown as Fig. 10; and if Ra is 3.2 um, the surface is shown as Fig. 11.

During the calculation, the peak value of Ra3.2 is one order of magnitude less than that of Ra6.3. Fig. 12 and Fig. 13 show the shape of Ra3.2.

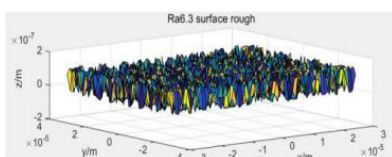


Fig. 10. Ra6.3 um

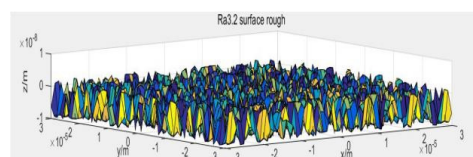


Fig. 11. Ra3.2 um

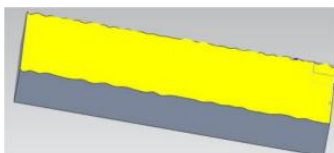


Fig. 12. Ra3.2 surface in UG

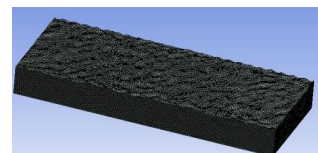


Fig. 13. Ra3.2 applied to guide rails

### 5. Mechanical and thermodynamic models

A dry contact model under different speeds was developed. With the ANSYS software, the transient temperature arising at the contact spots of two smooth or rough sliding surfaces was calculated, and the temperature distribution of discrete spots in the contact field, namely the temperature field under dry contact in the contact field was drawn.

Tribo-parts can be like these, the bolt is the moving part and the guide rail is the part that is a stationary component [11-14], shows as Table 1.

**Table 1.** Material properties of the gatling gun

25Cr2Ni4	Density	Thermal conductivity	Poisson
	7833	40	0.3
	Specific heat	Surface heat transfer coefficient	Coefficient of thermal expansion
	460.0	20	$1.5 \times 10^{-5}$

## 6. Results and discussion

### 6.1. Results of 6000 rpm at the smooth plane condition

The rail stress of the cam curve was analyzed in Fig. 14, thus the contact stress will up to 502.3 Mpa. And the displacement is shown as Fig. 15, and the temperature is shown as Fig. 16.

Then Table 2 shows the feature of the Gatling gun, which is only executed once.

**Table 2.** Performance comparison at the smooth plane condition

RPM	Stress / MPa	Displacement / mm	Temperature / °C
6000	502.3	0.0052524	86.258

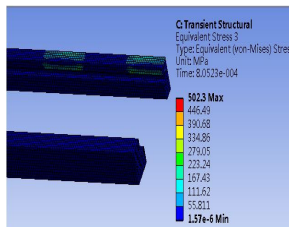


Fig. 14. The rail stress analysis

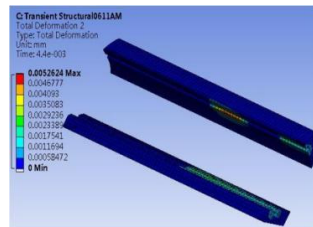


Fig. 15. The rail displacement analysis

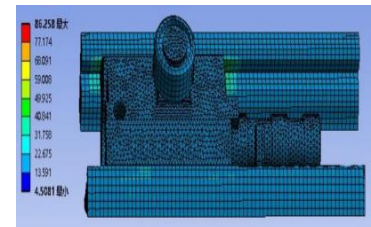


Fig. 16. The thermal situation

### 6.2. Result of Rpm 6000 at surface roughness

#### 6.2.1. States of Ra6.3

The rail stress of the cam curve was analyzed in Fig. 17, and the displacement is shown as Fig. 18. Then the Fig. 19 shows thermal situation of the general bolt and general guide rail.

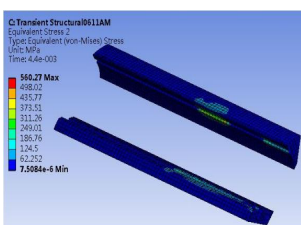


Fig. 17. Rpm 6000 and Ra6.3 the rail stress analysis

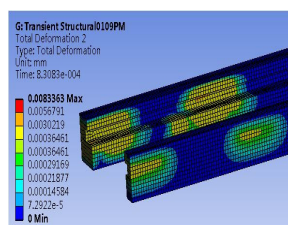


Fig. 18. Rpm 6000 and Ra6.3 the rail displacement analysis

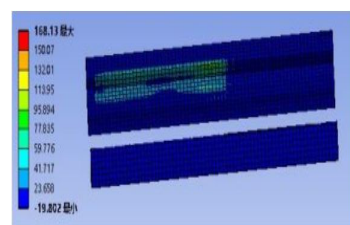


Fig. 19. Ra6.3 the general guide rail thermal situation

#### 6.2.2. States of Ra3.2

The rail stress of the cam curve was analyzed in Fig. 20, and Fig. 21 shows the displacement of the guide rail, and then Fig. 22 shows the thermal situation of the general bolt and general guide rail.

#### 6.2.3. Discussion

Then the Table 3 shows the feature of the Gatling gun Of 6000RPM, which is only executed

once.

The higher the firing rate, the lower the roughness of the guide rail on the Gatling gun. This way, even if the firing rate is higher, the friction heat temperature rise is not much, and the stress is uniform and not too large.

**Table 3.** Performance comparison at surface roughness of 6000 RPM

Ra	Stress / MPa	Displacement / mm	Temperature / °C
6.3	560.27	0.0083363	168.13
3.2	222.13	0.001	111.79

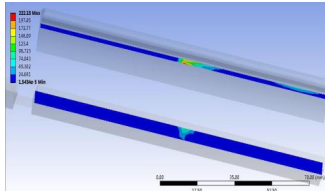


**Fig. 20.** The rail stress analysis with Ra3.2

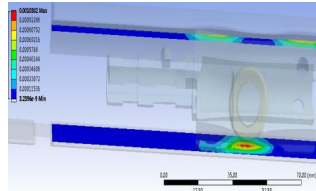


**Fig. 21.** The rail displacement analysis with Ra3.2

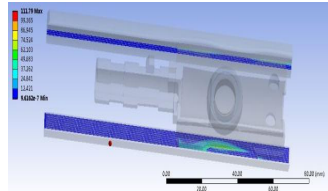


**Fig. 22.** Ra3.2 the general guide rail thermal situation

### 6.3. Result

The reduction of stress is:

$$\eta = \frac{560.27 - 502.3}{502.3} = 11.5 \%. \quad (4)$$

Using the power exponent [17] formula to describe the S-N curve of materials, calculate the fatigue life under a certain stress level:

$$\sigma^m N = C. \quad (5)$$

So the 6000 rpm of the flat condition is longer than the 6000 rpm of surface roughness with Ra6.3, but it's not as good as Ra3.2's. It plays an important role in improving the service life of friction surfaces.

The Stress state of Ra3.2 is much higher than that of Ra6.3 [18-19], with no significant difference in displacement, but the temperature has also dropped significantly, near 50 °C.

### 6.4. Discussion

It can be imagined that the more you shoot, the more you can reach a high level.

If the 10000 rpm, then the temperature is higher than the temperature of 8000 rpm. Maybe it may exceed 200 degrees.

Only once can we reach such a high level locally? When we experimented, we fired 30 rounds in a row. When we opened the gun box, my doctoral supervisor took an unlighted cigarette, took it close to the rotary body, and suddenly the cigarette caught fire.

### 7. Conclusions

1) With the increase of the shooting speed, the driving force is increased, so the stress, displacement, and temperature are increased. From a high firing rate to a low firing rate, the reduction of stress is preferred. Then the various states of the structure have reached a dangerous state, which makes it impossible to shoot for a long time at a higher firing rate. It plays an important role in improving the service life of friction surfaces.

2) A rotary gun with a lower firing rate can have a rough track and a high Ra value. For rotary weapons with higher firing rates, it is necessary to choose a smaller Ra value for the processing of trajectory.

## Acknowledgements

The authors are grateful to National Science Foundation of China Grant #51175481 and Open Research Fund Project of Key Laboratory of North University of China #2024.

## Data availability

The datasets generated during and/or analyzed during the current study are available from the corresponding author on reasonable request.

## Conflict of interest

The authors declare that they have no conflict of interest.

## References

- [1] Z. Liu, *The Theory and Design of Tribology*. Wuhan University of Technology Press, 2009, p. 62.
- [2] T. R. Thomas, *Rough Surfaces. Second Edition*. London: Imperial College Press, 1999, p. 60.
- [3] X. Jin, “Research Progress of High-Speed Wheel-Rail Relationship,” *Lubricants*, Vol. 10, No. 10, p. 248, Sep. 2022, <https://doi.org/10.3390/lubricants10100248>
- [4] F. Xia, C. Cole, and P. Wolfs, “The dynamic wheel-rail contact stresses for wagon on various tracks,” *Wear*, Vol. 265, No. 9-10, pp. 1549–1555, Oct. 2008, <https://doi.org/10.1016/j.wear.2008.01.035>
- [5] B. Wu, G. Xiao, B. An, T. Wu, and Q. Shen, “Numerical study of wheel/rail dynamic interactions for high-speed rail vehicles under low adhesion conditions during traction,” *Engineering Failure Analysis*, Vol. 137, p. 106266, Jul. 2022, <https://doi.org/10.1016/j.engfailanal.2022.106266>
- [6] W. J. Wang, P. Shen, J. H. Song, J. Guo, Q. Y. Liu, and X. S. Jin, “Experimental study on adhesion behavior of wheel/rail under dry and water conditions,” in *Wear*, Vol. 271, No. 9-10, pp. 2699–2705, Jul. 2011, <https://doi.org/10.1016/j.wear.2011.01.070>
- [7] C.-G. Lin, M.-S. Zou, C. Sima, S.-X. Liu, and L.-W. Jiang, “Friction-induced vibration and noise of marine stern tube bearings considering perturbations of the stochastic rough surface,” *Tribology International*, Vol. 131, pp. 661–671, Mar. 2019, <https://doi.org/10.1016/j.triboint.2018.11.026>
- [8] X. F. Yin, L. Wang, B. Kong, G. Song, and Y. Liu, “Probability analysis of the vibration of bridges with rough surface under stochastic traffic,” *International Journal of Structural Stability and Dynamics*, Vol. 18, No. 9, p. 1850108, Sep. 2018, <https://doi.org/10.1142/s0219455418501080>
- [9] J. Xu, Y. Bo, Q. Li, and X. Chang, “Research on main roller layout in bolt carrier for gatling gun,” *Acta Armamentariorum*, Vol. 31, No. 8, pp. 1035–1040, 2010.
- [10] D. J. Whitehouse and J. F. Archard, “The properties of random surfaces of significance in their contact,” *Proceedings of the Royal Society of London. A. Mathematical and Physical Sciences*, Vol. 316, No. 1524, pp. 97–121, Mar. 1970, <https://doi.org/10.1098/rspa.1970.0068>
- [11] R. Cross, “Effects of surface roughness on rolling friction,” *European Journal of Physics*, Vol. 36, No. 6, p. 065029, Nov. 2015, <https://doi.org/10.1088/0143-0807/36/6/065029>
- [12] J. Xu, Z. Yang, and Q. Li, “Solutions optimization of decreasing rail friction for bolts mechanical power consumption,” in *Journal of Physics: Conference Series*, Vol. 1303, No. 1, p. 012033, Aug. 2019, <https://doi.org/10.1088/1742-6596/1303/1/012033>
- [13] Y. Wang, L. Ren, and X. Yang, “Experimental study on the adhesion-decreasing and resistance-reducing characteristics of bionic materials with flexible and unsmoothed surfaces,” *Transactions of the Chinese Society of Agricultural Machinery*, Vol. 30, No. 4, pp. 1–4, 1999.
- [14] J. Xu, Q. Li, and Z. Yang, “Roller dynamic analysis and pure rolling criterion for one type high-speed cylinder cam mechanism,” *Journal of the Chinese Society of Mechanical Engineers*, Vol. 37, No. 4, pp. 315–323, 2016.
- [15] Y. Z. Hu and K. Tonder, “Simulation of 3-D random surface by 2-D digital filter and Fourier analysis,” *International Journal of Machine Tools and Manufacture*, Vol. 32, No. 32, pp. 82–90, 1999.

- [16] J. Xu, Y. Bo, and X. Chang, "New type of low power consumption cam curve designed for high fire ratio gatling gun," *Journal of Ballistics*, No. 2, pp. 70–73, 2009, [https://doi.org/1004-499x\(2009\)02-0070-04](https://doi.org/1004-499x(2009)02-0070-04)
- [17] L.-J. Ma, L.-C. Gu, and J. Chen, "Tribological properties of biomimetic rails based on ABAQUS," (in Chinese), *Modular Machine Tool and Automatic Manufacturing Technique*, pp. 97–119, 2015.
- [18] W.-T. Chang, L.-I. Wu, and C.-H. Liu, "Inspecting profile deviations of conjugate disk cams by a rapid indirect method," *Mechanism and Machine Theory*, Vol. 44, No. 8, pp. 1580–1594, Aug. 2009, <https://doi.org/10.1016/j.mechmachtheory.2009.01.002>
- [19] R. Stephens, *Metal Fatigue in Engineering, 2nd Edition*. Wiley-Interscience, 2000, pp. 17–20.